Comparison of Orion Vision Navigation Sensor Performance from STS-134 and the Space Operations Simulation Center

John A. Christian*
NASA Johnson Space Center, Houston, TX 77058

Mogi Patangan†
Jacobs Technology, Houston, TX 77058

and

Heather Hinkel,‡ Keiko Chevray,§ and Jack Brazzel**
NASA Johnson Space Center, Houston, TX 77058

The Orion Multi-Purpose Crew Vehicle is a new spacecraft being designed by NASA and Lockheed Martin for future crewed exploration missions. The Vision Navigation Sensor is a Flash LIDAR that will be the primary relative navigation sensor for this vehicle. To obtain a better understanding of this sensor's performance, the Orion relative navigation team has performed both flight tests and ground tests. This paper summarizes and compares the performance results from the STS-134 flight test, called the Sensor Test for Orion RelNav Risk Mitigation (STORRM) Development Test Objective, and the ground tests at the Space Operations Simulation Center.

I. Introduction

THE Vision Navigation Sensor (VNS) is the primary relative navigation instrument for the Orion Multi-Purpose Crew Vehicle (MPCV) being designed by NASA and Lockheed Martin (LM). This instrument, built by Ball Aerospace & Technologies Corporation (BATC), is a 256x256 Flash LIDAR that operates at an eye-safe wavelength of 1572 nm.[1] A prototype of the VNS was flown aboard the Space Shuttle Endeavour on STS-134 in May-June 2011 as part of the Sensor Test for Orion RelNav Risk Mitigation (STORRM) Development Test Objective (DTO).[2] After this flight test was completed, follow-up ground tests were performed using the STORRM VNS at the LM Space Operations Simulation Center (SOSC)[3,4] in Colorado where the Orion navigation team re-created the close-range portion of the STS-134 rendezvous trajectory. These re-creation tests were performed in August 2011. The SOSC is a state-of-the-art test facility equipped with a six degree-of-freedom (6-DOF) robot and a full size mockup of a portion of the International Space Station (ISS). The facility is large enough to allow for a complete re-creation of the last 60 m of the STS-134 rendezvous trajectory.

A. Background on Flash LIght Detection And Ranging (LIDAR) Sensors

The VNS is a Flash LIght Detection And Ranging (LIDAR) sensor – one of two common types of "Time-of-Flight (ToF) Cameras" available today. Unlike regular cameras that provide only intensity (i.e. brightness of reflected light) images, ToF Cameras are a class of sensors that provide both intensity and range information at each pixel location in the image. They accomplish this by measuring the time it takes for a light to travel from a source on the camera, to the target object, and back to the camera's receive optics. Therefore, the range at the *i*-th pixel, r_i, may be computed as (approximately),

$$r_i = \frac{c\, t_i}{2} \tag{1}$$

* Engineer, GN&C Autonomous Flight Systems Branch, and AIAA Member.
† GN&C Analyst, On-Orbit GN&C, Engineering & Science Contract Group.
‡ STORRM Principal Investigator, GN&C Autonomous Flight Systems Branch.
§ MPCV Orion Orbit GN&C System Manager, GN&C Autonomous Flight Systems Branch.
** MPCV Orion Orbit GN&C MODE Team Lead, GN&C Autonomous Flight Systems Branch.

where c is the speed of light and t_i is the light ToF measured at the i-th pixel location.

The light ToF may be measured in one of two primary ways. The first is to modulate a light source (typically in the near-infrared wavelength) and then demodulate the returning light using lock-in pixels as described in Ref. 5. This type of ToF Camera works well at short-range and has become popular in the robotics, digital entertainment, and automotive communities, but is not the type of ToF Camera used here. Instead, the VNS is one of a second type of ToF Camera that uses a single light pulse (rather than a modulated signal) – hence the name "Flash LIDAR". These type of sensors use a broad laser pulse (the "flash") that covers the entire sensor field-of-view (FOV) and each pixel measures the time between the common laser pulse transmission and when the return pulse is detected.

Therefore, the VNS (as a Flash LIDAR) generates two images at every measurement time: a 256x256 intensity image and a corresponding 256x256 range image. The most intuitive way to visualize this data is to plot the intensity image as a regular gray-scale image and the range image as a three-dimensional (3D) point cloud. An example of a VNS image is provided in Fig. 1.

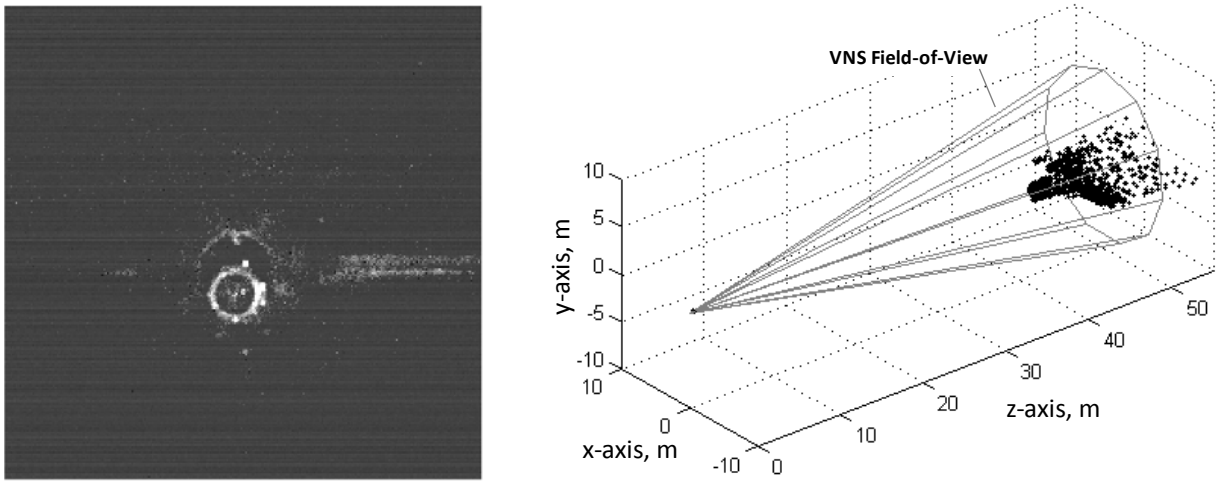

a) Intensity image. *b) Range image converted to 3D point cloud.*

Figure 1. Example VNS intensity image and range image collected during the STS-134 rendezvous with the ISS on 18 May 2011.

B. The VNS and its use on the Orion MPCV

In the case of the Orion MPCV, the VNS will be used for relative navigation with a cooperative target. In this context, the term "cooperative target" refers to a vehicle equipped with reflectors at known locations. When the VNS laser pulse arrives at the vehicle, the strongest return is generated at the locations of the reflectors. If one can detect the locations of these bright spots in the VNS intensity image, then range and bearing to each reflector may be obtained. This information may then be used for relative navigation. At long ranges, when only a few reflectors are visible, this data is incorporated into the Orion relative navigation filters. At close range, when many reflectors are visible (typically more than four), this data is used to directly compute relative pose (i.e. relative position and attitude).

C. Paper Outline

This paper focuses on comparing VNS results from the STS-134 STORRM flight test and the corresponding SOSC ground test that attempted to re-create the on-orbit rendezvous trajectory/conditions. Therefore, the paper will begin with a brief review of the STORRM DTO in Section II, followed by a description of the SOSC facility in Section III. Then, a brief summary of the common VNS data processing techniques used to process both STORRM data and SOSC data is presented in Section IV. Results are then presented for STORRM and the SOSC in Section V and Section VI, and then compared directly in Section VII.

II. Overview of STORRM DTO on STS-134

The Sensor Test for Orion RelNav Risk Mitigation (STORRM) Development Test Objective (DTO) flew aboard the Space Shuttle Endeavour on STS-134 in May-June 2011. STORRM was designed to characterize the performance of the VNS (Flash LIDAR) and docking camera (DC) being developed for the Orion MPCV. In addition, STORRM was designed to collect data from these sensors to mitigate the loss-of-mission risk in upcoming Orion test flights and to increase the technology readiness level (TRL) of these sensors. The VNS will be the primary navigation instrument used by the Orion vehicle during rendezvous, proximity operations, and docking (RPOD) starting at 5 km from the target vehicle. To accomplish these goals, the VNS and DC were placed in the STORRM Sensor Enclosure Assembly (SEA). The SEA was then mounted in the Shuttle payload bay directly next to the Shuttle's Trajectory Control Sensor (TCS), a scanning LIDAR system used during proximity operations. A Best Estimated Trajectory (BET) utilizing TCS measurements served as the "truth" for VNS post-flight analysis. STORRM data collection opportunities took place on Flight Day 3 (FD3) during rendezvous and docking to the ISS and Flight Day 15 (FD15) during undock, flyaround, re-rendezvous and final separation. The re-rendezvous, designed to mimic the planned Orion rendezvous profile, was a first-ever for the Shuttle.[6] A detailed discussion of the STORRM mission phases and concept of operations is provided in Ref. 2. Throughout all of these mission phases, data from the STORRM VNS was produced and recorded at a rate of 30 Hz. This data was then combined during post-flight analysis to produce reflector range and bearing measurements at a rate of either 1 Hz or 5 Hz. More specifically, the range and bearings at each measurement time were generated through a new centroiding algorithm designed to deal directly with reflectors in Flash LIDAR imagery (see Section IV).

The prototype VNS tested during the STORRM DTO had eight different range bins (using the phonetic alphabet, these are referred to as range bins Alpha through Hotel). This paper deals primarily with the close-range portion of the trajectory that could be simulated in the SOSC (closest 60 m). Therefore the results shown in this report focus on data collected in range bin Golf and range bin Hotel.

On a previous Shuttle mission, five reflectors, specially designed to be highly reflective in the VNS laser wavelength, but opaque in the TCS and visible wavelengths, were installed on the ISS visual docking target for use during close-range STORRM operations. The STORRM reflector pattern is as shown in Fig. 2.

Some of the challenges with ground based testing of the VNS that motivated the STORRM DTO included: the dynamic nature of the proximity operations trajectory, adequate long-range testing in both static and dynamic conditions, variations in LIDAR performance when operating in an atmosphere (instead of the vacuum of space), and accurate simulation of the reflective environment in the VNS wavelength around the ISS.

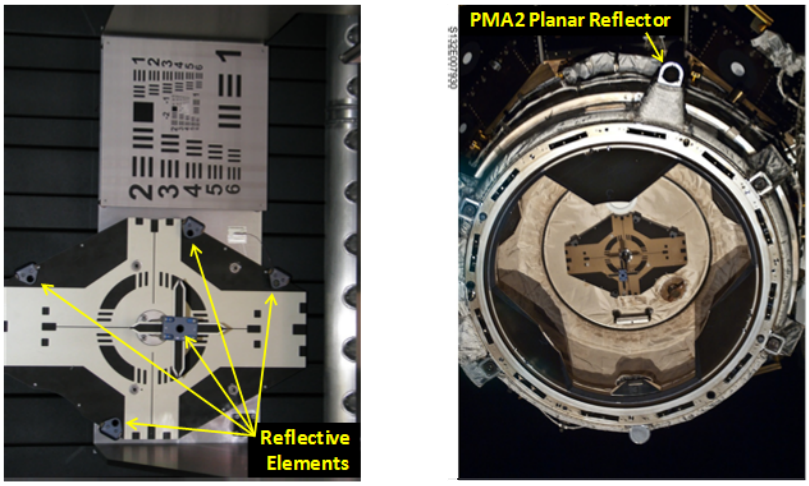

a) Approximate location of STORRM reflectors on docking target.

b) Image taken during STS-132 of docking target in PMA2 after installation of STORRM reflectors.

Figure 2. ISS Pressurized Mating Adapter 2 (PMA2) docking target after addition of the five STORRM reflectors.

The STORRM DTO provided valuable insight into the on-orbit performance of the VNS, and provided confidence that the VNS will satisfy requirements and perform as expected for Orion. STORRM was extremely successful and met nearly all objectives for the flight test. Flight Test Objectives were split into both in-flight and post-flight categories. Post-flight objectives were those which involved performing necessary steps on raw VNS range and intensity images to use with algorithms. Orion engineers analyzed over 380 GBytes VNS data. The data provided a great advancement in the Orion teams' understanding of how to use the VNS for relative navigation in a space environment.

Test Objectives were identified for different ranges of data collection, however, since this paper addresses the comparison of STORRM to SOSC testing, only the close-in objectives are shown Table 1. The grayed rows in the table represent upcoming work for Orion and won't be addressed until a future date. A number of other items were studied after STORRM outside the flight test objectives as well. These items fell into the following categories: VNS performance, thermal conditions of STORRM components, VNS function/settings and their effects, photogrammetry results of the reflective elements, and VNS-based best estimated trajectory.

Table 1. Summary of close-range VNS test objectives for STORRM DTO. Requirements highlighted in gray were deferred.

Flight Phase	#	VNS Objective	Objective*	Met	Partially Met	Not Met
Final Approach/ Separation Flight Test Objectives (50 m– Dock)	V08P	Allow for overlap with ground testing facilities	P	X		
	V09P	Collect data to support pose calculation	P	X		
	V10P	Characterize the ISS PMA2 augmented docking target	P	X		
Final Approach/ Separation Post-Flight Objectives (50 m– Dock)	V04S	Perform calculations on raw data to determine pose	S			
All Flight Phases Post-Flight Objectives	V11P	Perform calculations on raw data to determine geometric centroids to reflective elements	P	X		
	V12P	Perform calculations on raw data to determine range and horizontal/vertical angles to target	P	X		
	V13P	Compare VNS measurements with Orbiter sensors and relative best estimated trajectory	P	X		
	V14P	Characterize noise and bias	P	X		
	V15P	Incorporate data into Orion simulations to assess filter performance	P			
	V16P	Investigate any anomalous data collected	P	X		
	V17P	Update ground models as appropriate	P			

* P = Primary, S = Secondary

III. Re-creating the STORRM DTO in SOSC

A. Overview of the Space Operations Simulation Center (SOSC)

The LM Space Operations Simulation Center (SOSC) at the LM Waterton Campus in Littleton, Colorado, includes the Autonomous Rendezvous and Docking Facility (ARDF). Images of the SOSC are provided in Fig. 3. The ARDF was established with LM Space Systems Company (LMSSC) investment funding to support development testing, characterization, and risk reduction activities.

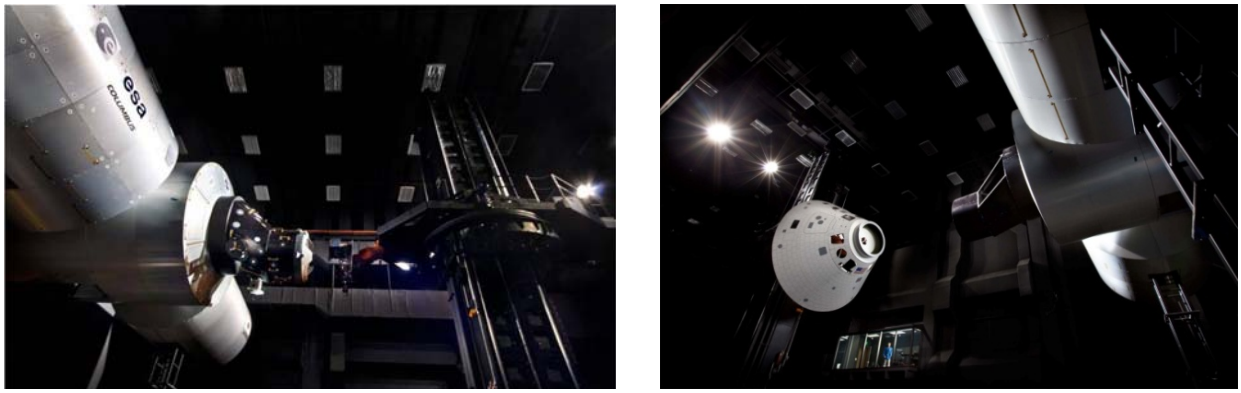

Figure 3. The Space Operations Simulation Center (SOSC) with the ISS mockup.

The ARDF consists of elements of the SOSC, including: a full size mockup of the ISS (consisting of Node 2, Columbus module, Kibo module, and PMA2), full size mockup of the Orion Crew Module (CM), docking interface hardware, and associated support hardware (ISS support structure and CM Cradle). The SOSC consists of a high bay with maximum sensor-to-target effective range of 60 m and dual 6-DOF motion simulators. It contains four Mission Operations Centers (MOCs) with connectivity to the dual high bay control rooms and data/video interface room. The high bay is rated at Class 300,000 ($\geq$ 0.5 μm maximum particles/m^3) cleanliness and includes orbital lighting simulation capabilities.

Within the SOSC, there are two rail-mounted 6-DOF robot mechanisms for use in simulating docking vehicles. The larger of the 6-DOF robot mechanisms is supported on three rails, and the second, smaller mechanism is supported on two rails. Also, the facility supports three fixed target structures situated throughout the testing area.

The testing area is 60 meters long and 15.2 meters wide by 15.2 meters tall, thus allowing a great amount of freedom of movement, and large-scale, flight-like simulations of proximity maneuvers and docking events. The facility also has two apertures for access to external extended-range outdoor target test operations.

The SOSC support software is hosted on a network of computers at the SOSC. A suite of software was used during the SOSC testing to drive the robot as well as process VNS data.

B. Overview STORRM Re-Creation Test

The primary objective of the STORRM re-creation test was to characterize the SOSC environment in comparison to the ISS flight environment, as captured by the STORRM DTO flown on STS-134. The SOSC robot was programmed to fly the same trajectory as flown for STS-134 for the final 60 meters (based on the STS-134 BET) and data was collected from the VNS. The VNS data from the SOSC re-creation test were then compared against the VNS data from the STORRM flight.

Specific objectives of this test included the following:

- Characterize the SOSC environment in comparison to the ISS flight condition, as captured by the STORRM DTO.
- Show that the VNS produces similar results, within tolerance, with respect to intensity returns for the specific targets (TCS reflectors and STORRM reflectors) and range and bearing measurements to centroids, in ground testing as received during the STORRM DTO. If VNS results differ from the flight data, document the differences and identify possible causes.

The SOSC re-created the STS-134 final approach and undock in order to evaluate the facility test resources (motion control, ISS mockup target environment, lighting, etc.) in providing a space-like environment for future Orion testing. Recall that the STORRM DTO flew an Orion VNS and DC housed together in the SEA. The demonstration that the SOSC successfully simulated the final approach and undock segments of the STORRM flight condition by flying the STORRM flight hardware (specifically the SEA) in the same configuration, on the same trajectory, and in a similar environment as executed during the STORRM DTO.

Some of the specific tasks necessary for execution of this test included the following:

- Develop the necessary interfaces to operate the VNS in the SOSC facility.
- Develop a core capability to test the VNS and analyze results.

IV. Processing VNS Images

Recall that the VNS, as a Flash LIDAR, produces an intensity image and a range image at each measurement time. For these images to be useful for cooperative relative navigation, they must be searched for reflectors. Therefore, the primary VNS image processing task is to develop an algorithm that can produce a list of reflector centroids while being robust to spurious reflections and sensor noise. As may be seen from Fig. 4, actual VNS images of the ISS contain many spurious reflections at close range and the importance (and difficulty) of reliable reflector detection and identification in this environment cannot be overstated.

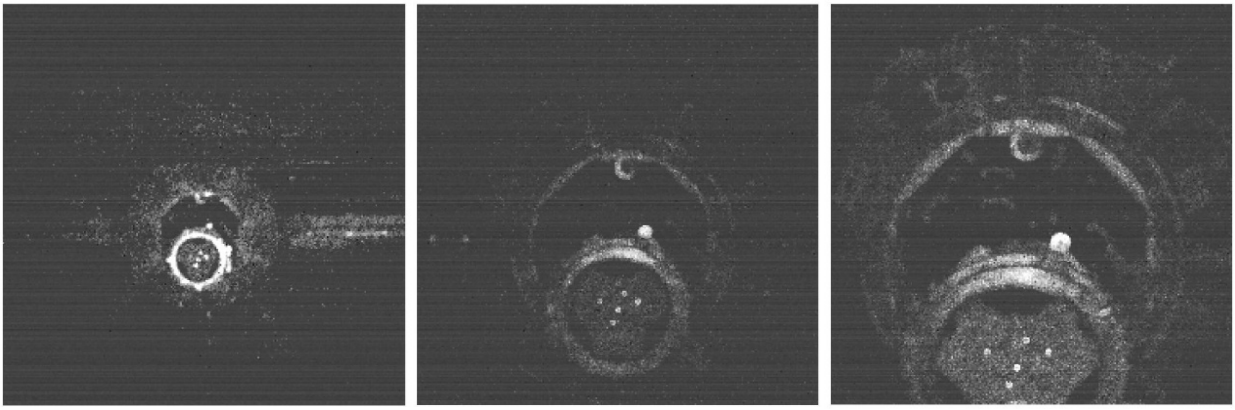

a) Port-to-port range of 28.7 m *b) Port-to-port range of 11.4 m* *c) Port-to-port range of 6.5 m*

Figure 4. Example VNS images of the PMA2 clearly show strong returns from ISS components that are not reflectors.

After attempting numerous reflector finding algorithms (ranging from simple thresholding to template matching), the best results were achieved using techniques based on mathematical morphology. More specifically, the approach begins by convolving the raw intensity image with a negative Laplacian of Gaussian filter and keeping only the pixels whose processed intensity is above some threshold. Then, using both the raw and filtered intensity image, the pixels belonging to candidate reflectors in each individual VNS frame are identified using a combination of image reconstruction[7] and attribute openings.[8] Depending on the range to the target, a varying number of VNS frames may be accumulated to check for the persistence of candidate reflectors. After the accumulation is complete, each candidate reflector must pass checks on size, intensity, and shape to be added to the list of reflectors for that frame. At close range, such as the data presented in this paper, processed centroids are produced at a rate of 5 Hz. For both STORRM and the SOSC, centroids were produced as a post-flight (or post-test) data product. These algorithms were not run in real-time here, although other efforts are underway to extend these techniques for real-time applications.

Given a set of pixels belonging to a specific (i-th) reflector, the centroid coordinates of that reflector, $[u_c,v_c]_i$, is computed using a simple center-of-mass algorithm. Mathematically,

$$(u_c)_i = \frac{1}{W} \sum_{(u,v)\in B_i} u\, J(u,v) \tag{2}$$

$$(v_c)_i = \frac{1}{W} \sum_{(u,v)\in B_i} v\, J(u,v) \tag{3}$$

where $J(u,v)$ is the processed intensity at the coordinate $[u,v]$, B_i is the set of pixels belonging to the i-th candidate reflector, and

$$W = \sum_{(u,v)\in B_i} J(u,v) \tag{4}$$

Additionally, the range to each candidate reflector is obtained by taking the median range value of the pixels in the set B_i whose raw intensity is above some minimum value. A minimum intensity is required to ensure that the laser return was strong enough to produce a reliably valid range measurement.

It is important to note that there are many different ways to find reflectors and compute centroids given identical VNS imagery. For example, a fundamentally different algorithm (that performs an identical reflector finding and centroiding task) has been developed by the vendor, and this other algorithm was used to generate the centroid results shown in Ref. 9.

V. VNS Performance During the STORRM DTO on STS-134

Over 380 GBytes VNS data were collected on-orbit during STS-134. Orion relative navigation engineers processed all of this data and produced centroid time histories for each flight phase using the VNS processing techniques outlined in Section IV. As an example, a summary of these observed reflector centroids over the entire FD3 rendezvous is presented in Fig. 5 and Fig. 6. The black vertical lines in these images denote the locations of range bin transitions (Alpha to Hotel from left to right). The spreading of the $[u,v]$ coordinate of reflectors in Fig. 5 occurs as the range approaches zero because the ISS appears larger in the image. The apparent noisiness of the close range data is largely a plotting artifact, and the reader is referred to Fig. 7 through Fig. 10 for a better representation of the close-range centroid behavior.

Focus is now turned to the two closest range bins, Golf and Hotel, for the purposes of direct comparison with data collected in the SOSC. In addition to just the centroids found in the VNS images, the expected reflector locations were predicted using the STS-134 BET. Figure 7 through Fig. 10 show both the observed centroids and the expected reflector locations on a single plot. The x-axis for each plot denotes the docking port (ISS) to docking port (Orbiter) range decreasing from left to right. When looking at the range plots, note that the reflectors (both the PMA2 planar and the five STORRM reflectors) are recessed from the docking ring (see Fig. 2.a) – meaning that the measured range should be a little larger than the port-to-port range.

There are a few items of particular note in the STS-134 flight data. First, for a large portion of range bin Golf, a strong reflector-like return was observed from a reflection off the window of a Soyuz module docked to the ISS. This was consistently reported as a centroid from the reflector finding algorithm until it became obscured by the ISS truss at a range of about 46 m. Second, the close-range (within 50 m) ISS PMA2 reflective environment is dominated by VNS laser returns from four different sources:

1. PMA2 planar reflector
2. STORRM reflectors 1-5
3. Spurious returns from the docking ring
4. Spurious returns from other ISS elements

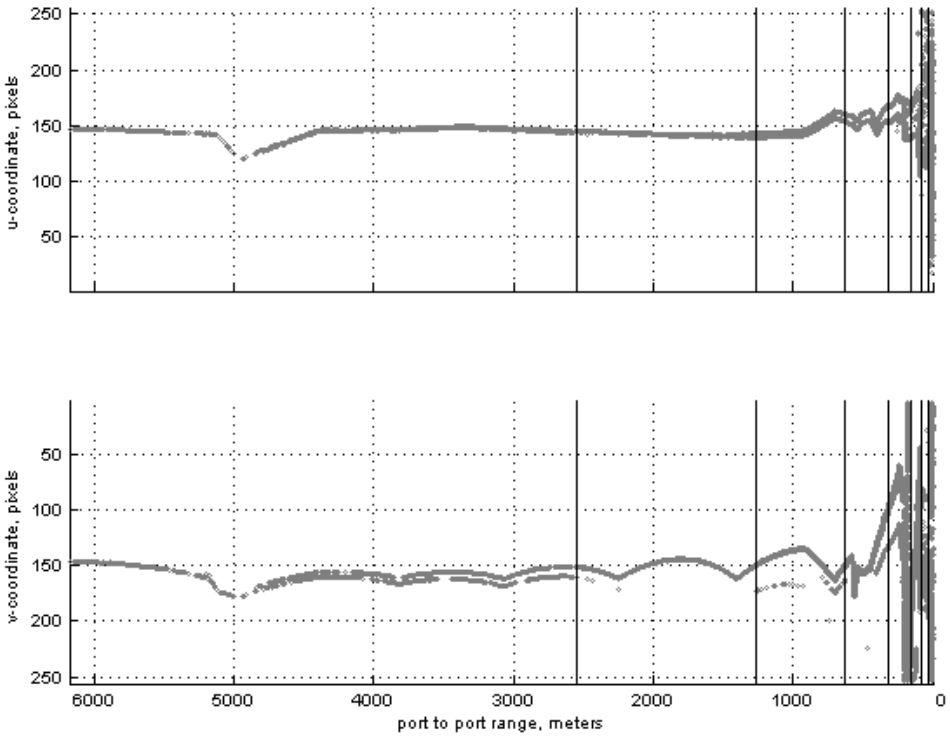

Figure 5. Observed centroid [*u*,*v*] coordinates in VNS imagery from STS-134 FD3 rendezvous. Black vertical lines represent range bin transitions.

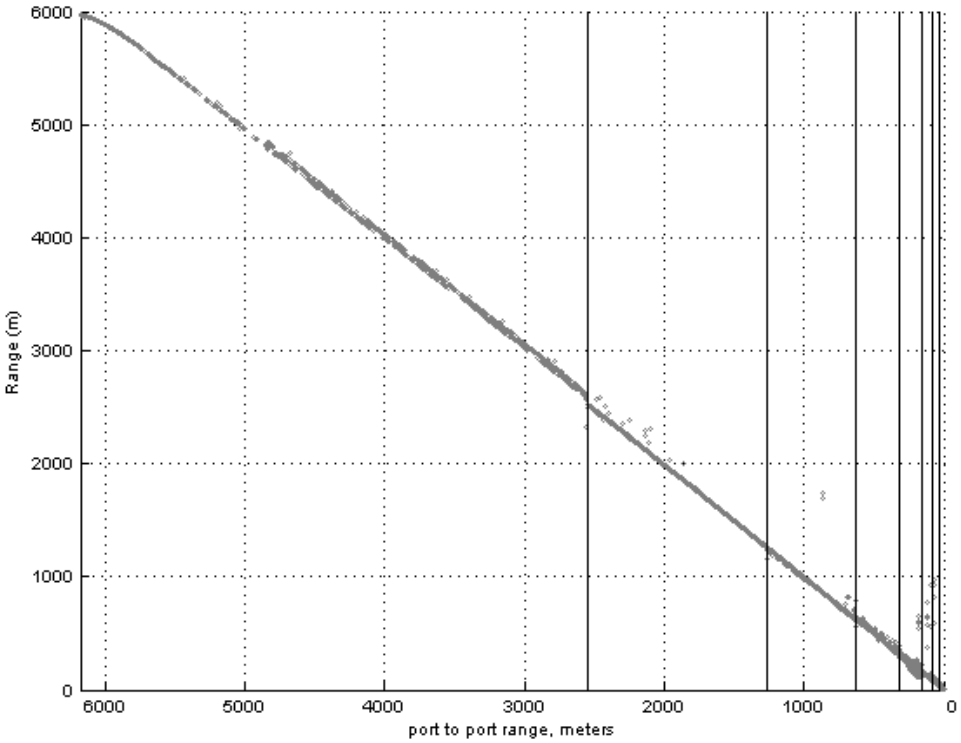

Figure 6. Observed centroid ranges in VNS imagery from STS-134 FD3 rendezvous. Black vertical lines represent range bin transitions.

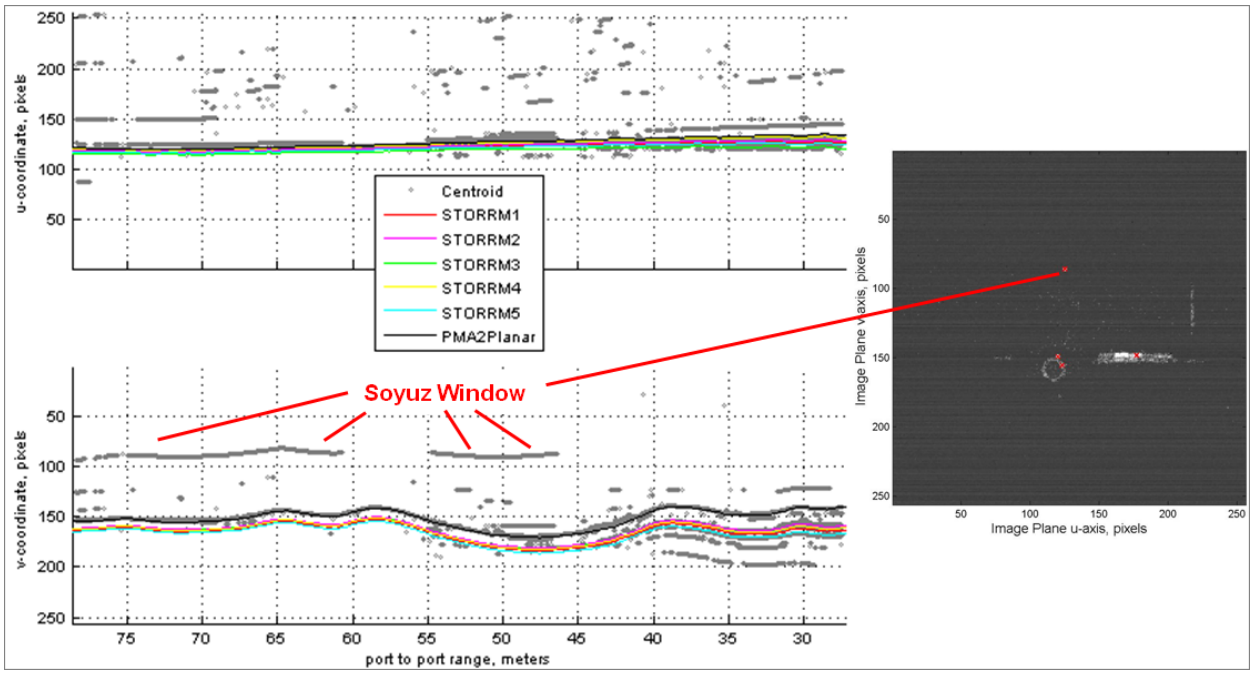

Figure 7. Time history of centroid [*u*,*v*] coordinates from STS-134 docking: range bin Golf.

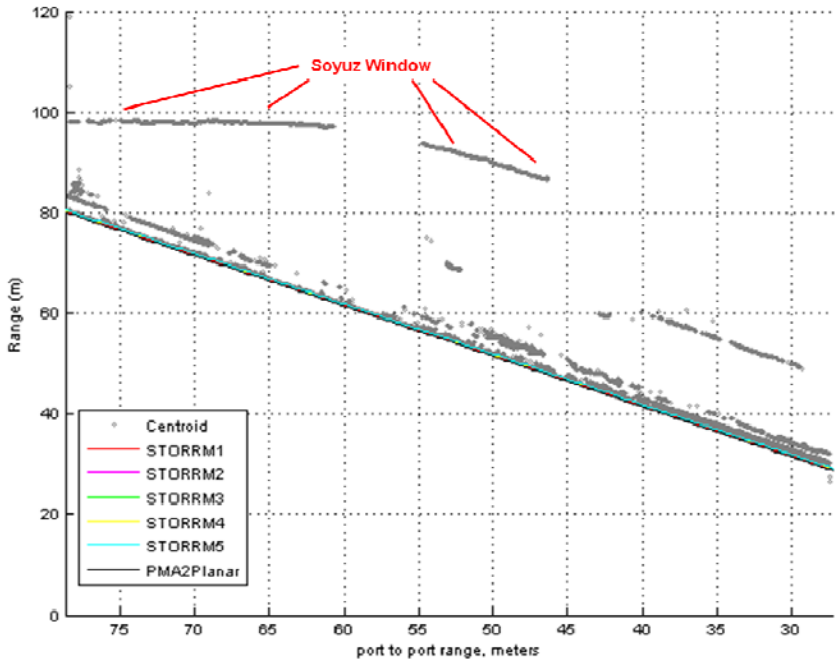

Figure 8. Time history of centroid ranges from STS-134 docking: range bin Golf.

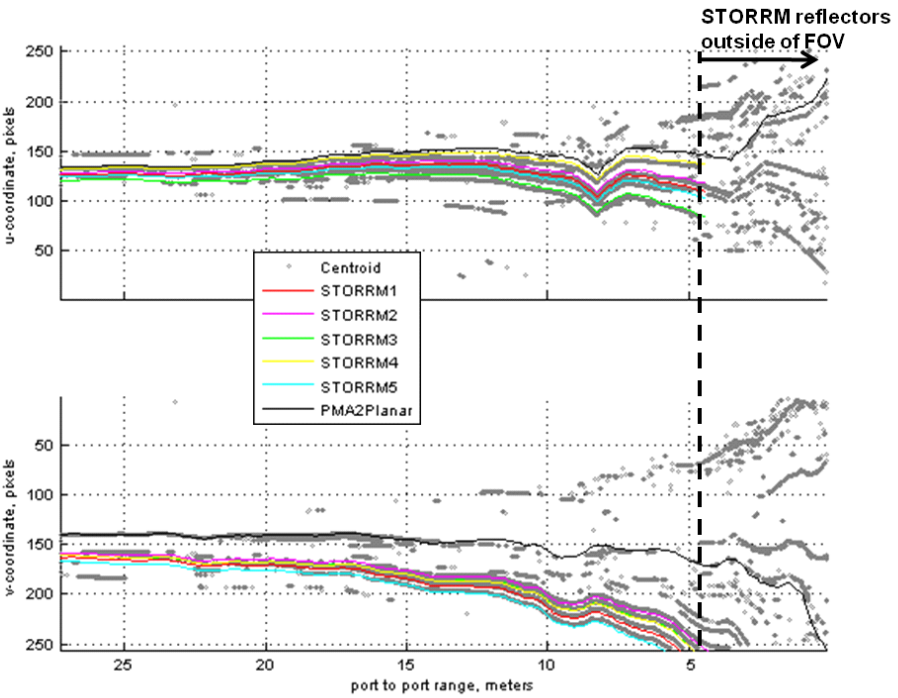

Figure 9. Time history of centroid [*u*,*v*] coordinates from STS-134 docking: range bin Hotel.

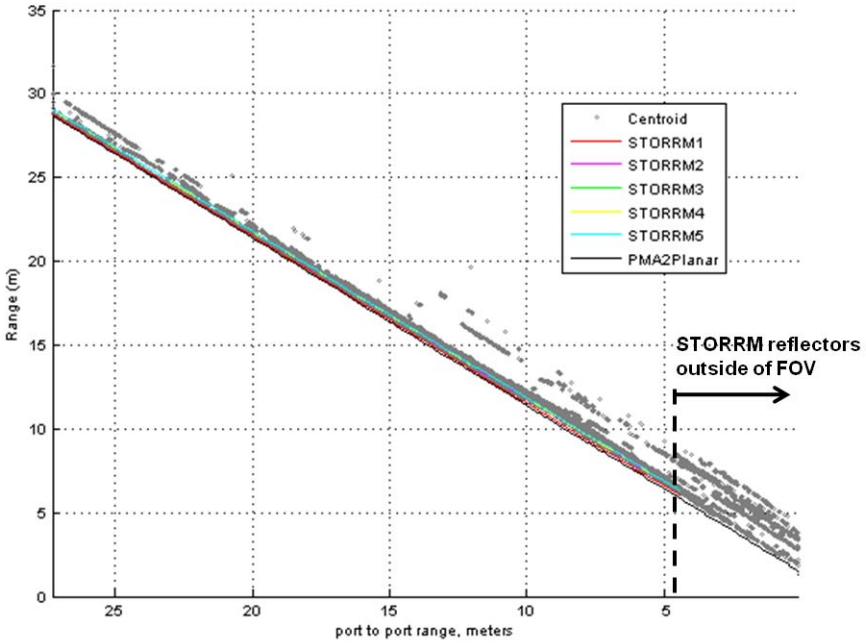

Figure 10. Time history of centroid ranges from STS-134 docking: range bin Hotel.

The spurious reflections described in #3 and #4 (of the list on the bottom of pg. 7) can be quite problematic, and are the primary source of complications in autonomously finding reflectors. Looking at the VNS images (see Fig. 4 and Fig. 17), it is immediately evident that the spurious reflections can be as bright (or brighter) than the reflectors, rendering many simple reflector finding algorithms inadequate. One of the great challenges moving forward will likely be our ability to implement more sophisticated algorithms that are also able to reliably produce centroids at 5 Hz on the available flight processors.

The docking ring clearly exhibits characteristics of both diffuse reflection and specular reflection. The diffuse component is evident when portions of the docking ring near the edge of the VNS FOV (approximately 10 degree incidence angle) continue to give significant returns. The specular component explains why portions of the docking ring near the center of the image (near the VNS boresight and at a low incidence angle) appear very bright in the VNS intensity image. Strong reflections from the docking ring will likely be a larger problem for Orion because the docking ring will be centered in the image (and, therefore, at a low incidence angle) during most of the final approach. That being said, it is only at very close ranges that the docking ring becomes a significant factor. At ranges beyond about 35 m, the PMA2 planar reflector consistently has an intensity return noticeably larger than the docking ring. At ranges within 35 m, however, the maximum intensity return from the docking ring is on the same order of magnitude as the maximum returns from the PMA2 planar reflector and the STORRM reflectors.

VI. VNS Performance at the Space Operations Simulation Center

After completion of STS-134, the STORRM SEA was shipped from the NASA Kennedy Space Center (KSC) to the SOSC facility. Over the summer of 2011, the Orion relative navigation team worked with SOSC engineers to improve the fidelity of the ISS mockup in the VNS wavelength and to integrate the STORRM VNS with the SOSC. Then, in August 2011, the last 60 m of the STS-134 FD3 rendezvous trajectory was re-created in the SOSC. The position and attitude of the robot that moved the VNS was driven by the STS-134 BET.

A. Test Set-up and Configuration

The SOSC STORRM re-creation test involved the last 60 m of the STS-134 rendezvous, which included a portion of range bin Golf and all of range bin Hotel. This test used the same on-orbit VNS settings that were used during STS-134 FD3 rendezvous. The primary difference in VNS settings between range bins Golf and Hotel was a switch from a higher to a lower gain setting, which was done to avoid image oversaturation due to the increase of returned energy from specular surfaces. The switch between range bins in the SOSC was accomplished by triggering the switch at the robot arm waypoint that corresponded to the BET data point when the on-orbit switch occurred.

To re-create the Orbiter-ISS docking environment, the STORRM reflectors and PMA2 Planar reflector were installed on an ISS mockup at one end of the SOSC facility and the STORRM VNS was mounted on a robotic arm. The robotic arm could be maneuvered using the STS-134 BET, although the BET had to be transformed into the SOSC facility reference frame. The reflector locations were surveyed with respect to the SOSC facility reference frame. SOSC personnel provided the VNS camera frame location (x, y, and z) and attitude (pitch, yaw, and roll) with respect to the SOSC facility reference frame at a rate of 83.3Hz. Figure 11 shows the trajectory of the VNS camera frame in the SOSC facility.

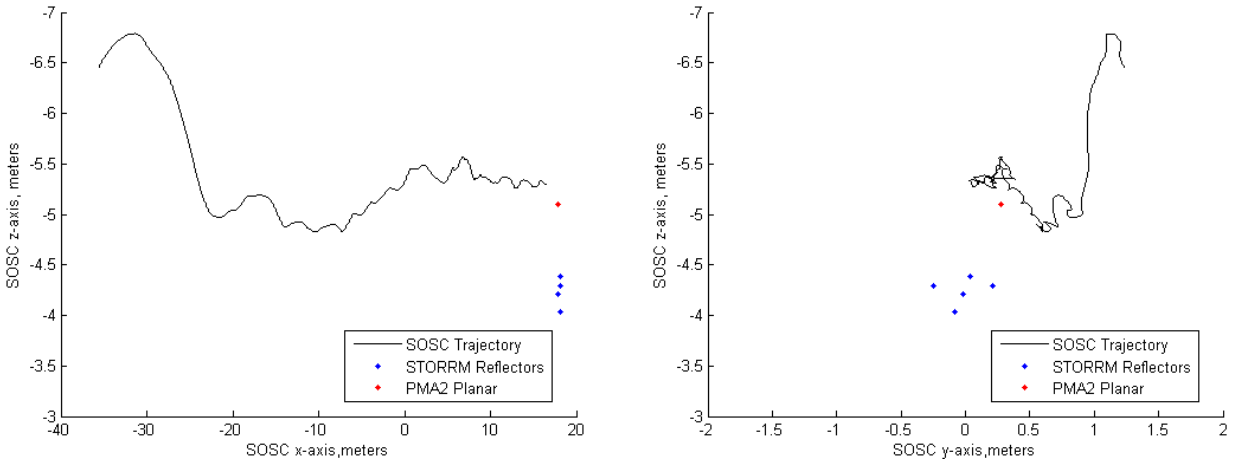

a) x-z projection *b) y-z projection*

Figure 11. VNS camera frame trajectory in the SOSC facility reference frame.

B. Observed Centroid and Expected Reflector Location Overlay

The centroids observed in the VNS imagery obtained during the entire rendezvous re-creation test in the SOSC were computed using the techniques described in Section IV. The expected reflector [*u*,*v*] coordinates were generated by projecting the BET-predicted reflector locations onto the VIN image plane using a simple pinhole camera model.[10]

Figure 12 through Fig. 15 are plots of the centroid pixel locations and range overlaid with the expected reflector locations for the STORRM reflectors and the PMA2 Planar. Figure 12 and Fig. 13 correspond to data collected during range bin Golf, while Fig. 14 and Fig. 15 show data collected during the range bin Hotel. The x-axis for each plot denotes the docking port (ISS) to docking port (Orbiter) range decreasing from left to right. The docking port locations were imaginary points in the SOSC facility and were calculated from a surveyed location (i.e. PMA2 Planar) by using their known structural locations on the ISS and Orbiter, respectively. The plots show good agreement between the centroids and the expected reflector locations.

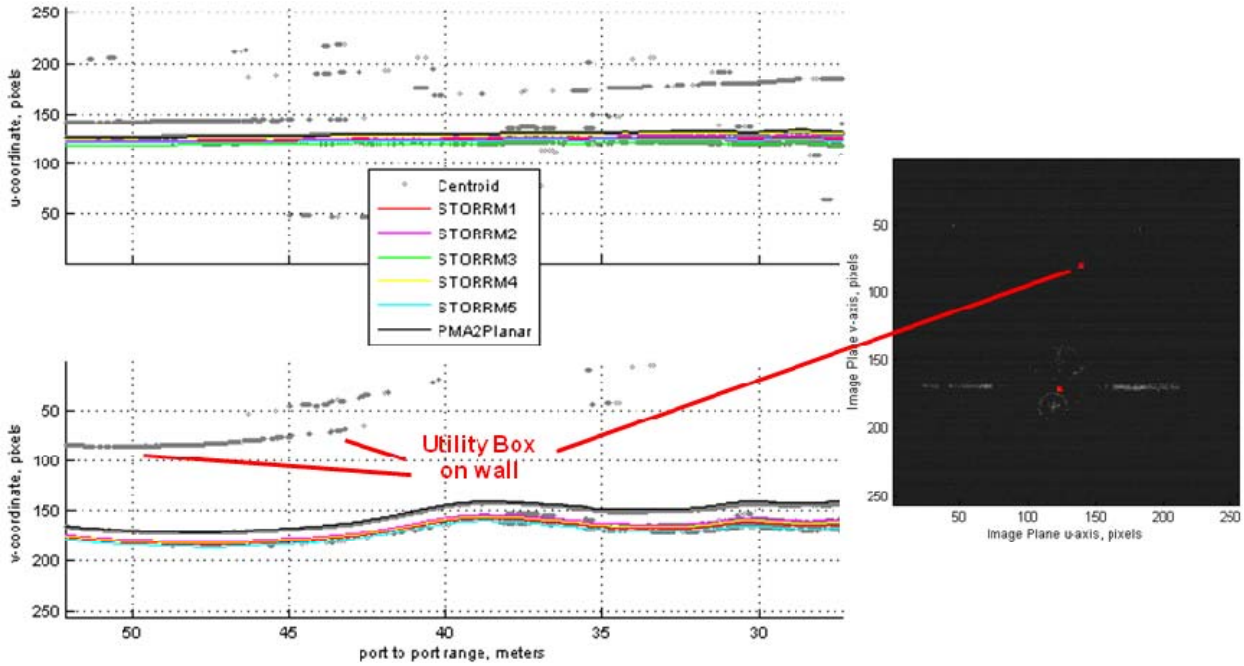

Figure 12. Time history of centroid [*u*,*v*] coordinates from SOSC docking: range bin Golf.

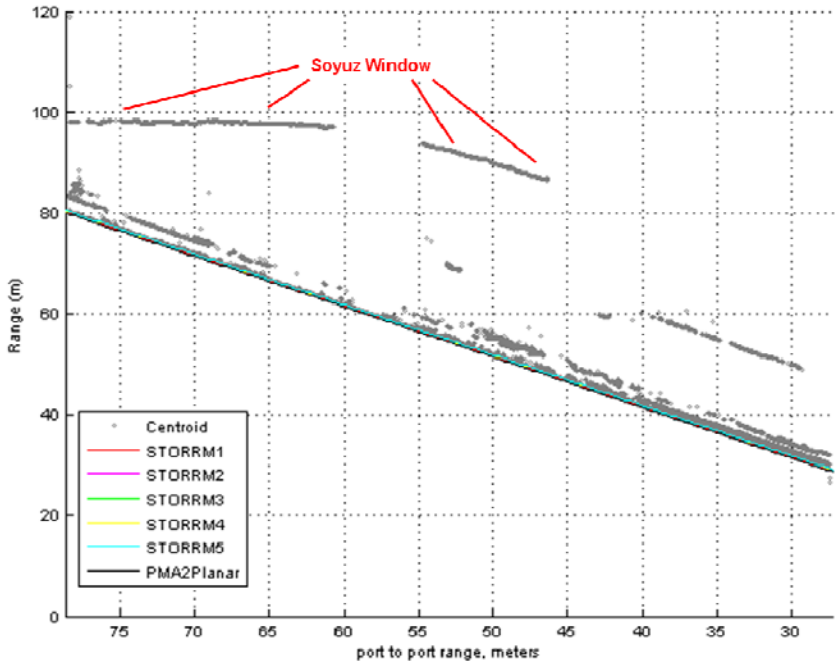

Figure 13. Time history of centroid ranges from SOSC docking: range bin Golf.

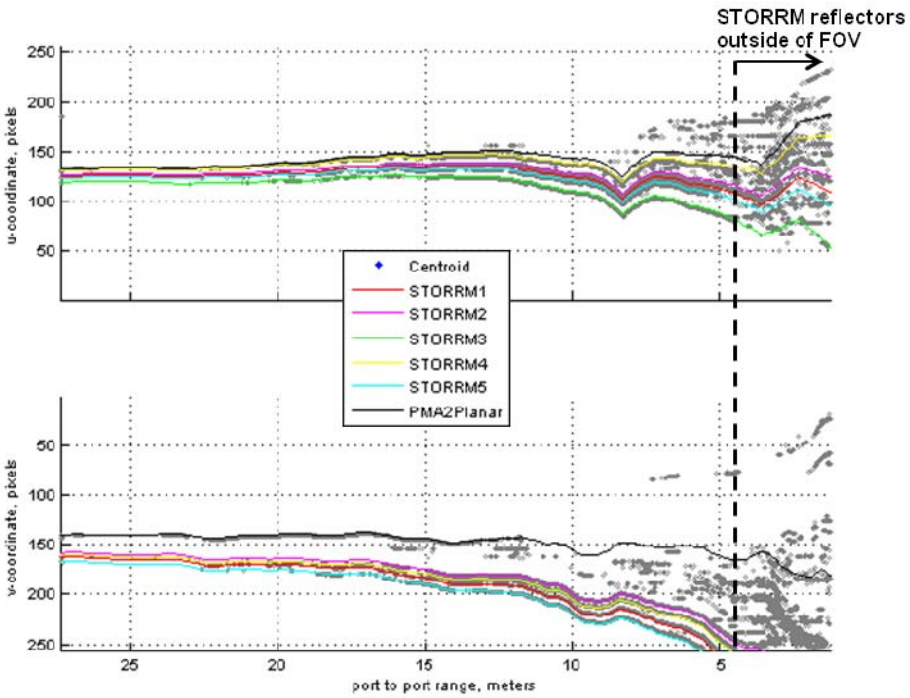

Figure 14. Time history of centroid [*u*,*v*] coordinates from SOSC docking: range bin Hotel.

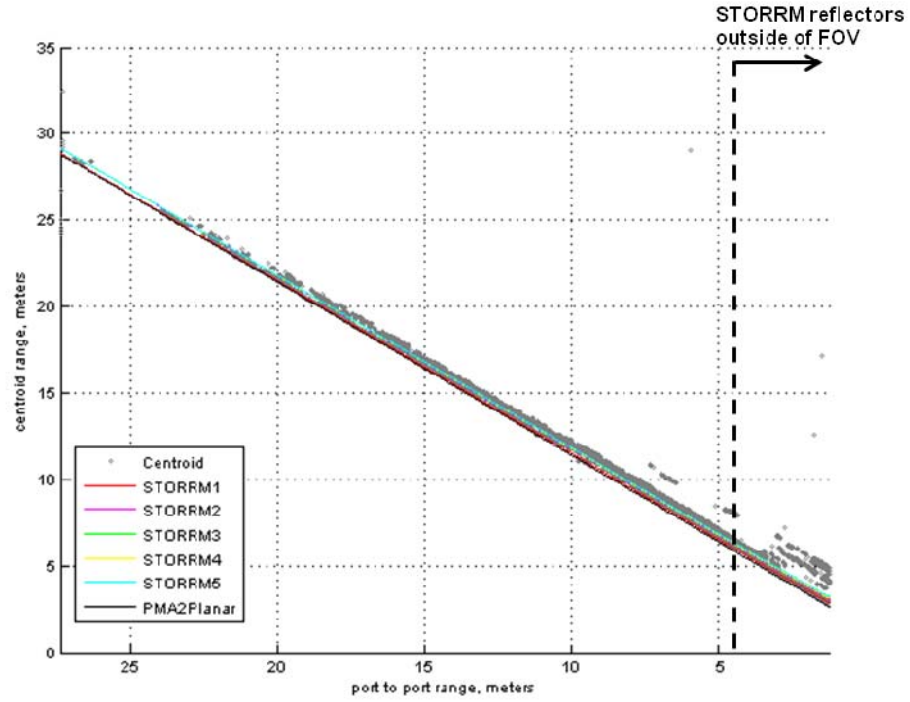

Figure 15. Time history of centroid ranges from SOSC docking: range bin Hotel.

VII. Comparison of STS-134 and SOSC Results

Now that each individual data set has been presented individually, they may be viewed side-by-side and assessed for similarities and differences. As a quick first-cut assessment, a comparison of Fig. 7 through Fig. 10 (STS-134 centroids from Section V) with Fig. 12 through Fig. 15 (SOSC centroids from Section VI) shows excellent agreement between these two data sets. Now, digging a little deeper, a few observations are in order.

First and foremost, similar centroiding performance of the PMA2 planar reflector and the five STORRM reflectors was observed on-orbit and in the SOSC. An example comparison of centroid results is shown in Fig. 16. Both data sets show that the VNS begins to lose the PMA2 planar at 12-13 m, while beginning to reliably pick out the STORRM reflectors at 15-20 m. This is good, because similar reflector behavior and centroiding results between data collected on-orbit and in the SOSC is absolutely critical if the facility is to be used to predict vehicle navigation performance.

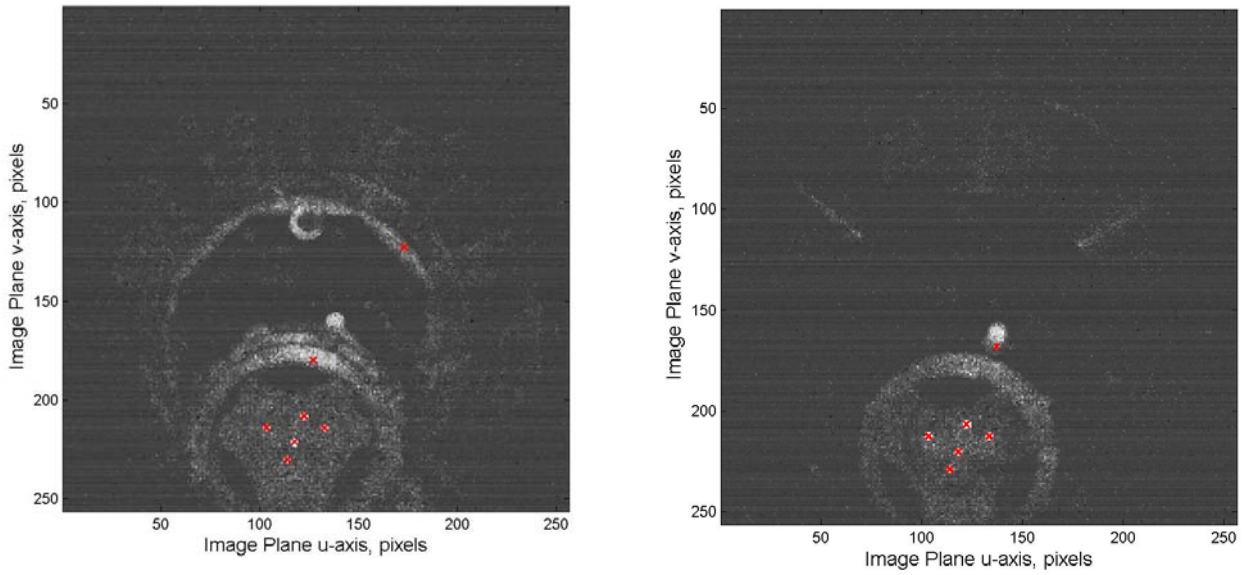

a) STORRM data from STS-134 FD3 rendezvous *b) Simulated rendezvous in SOSC*

Figure 16. Comparison of STS-134 flight data (left) with SOSC ground test data (right). Red "x" indicates automatically identified reflector centroid locations.

Second, the SOSC represents a noticeably cleaner reflective environment than the actual ISS. This is evident from side-by-side comparison of intensity images (see Fig. 17) or by comparing the number of spurious reflections (centroids not corresponding to expected reflector locations) in Fig. 9 and Fig. 14. This difference persists despite a significant amount of effort to modify the ISS mockup in the SOSC to more accurately simulate the returns experienced on-orbit. The dominant spurious reflection was clearly the docking ring. Therefore, the intensity of the docking ring, compared to the intensity of the PMA2 planar and the five STORRM reflectors, was computed for both STS-134 and the SOSC. The results are shown in Fig. 18. Although a significant improvement from the initial mockup configuration, the docking ring in the SOSC consistently exhibited dimmer returns than seen on-orbit.

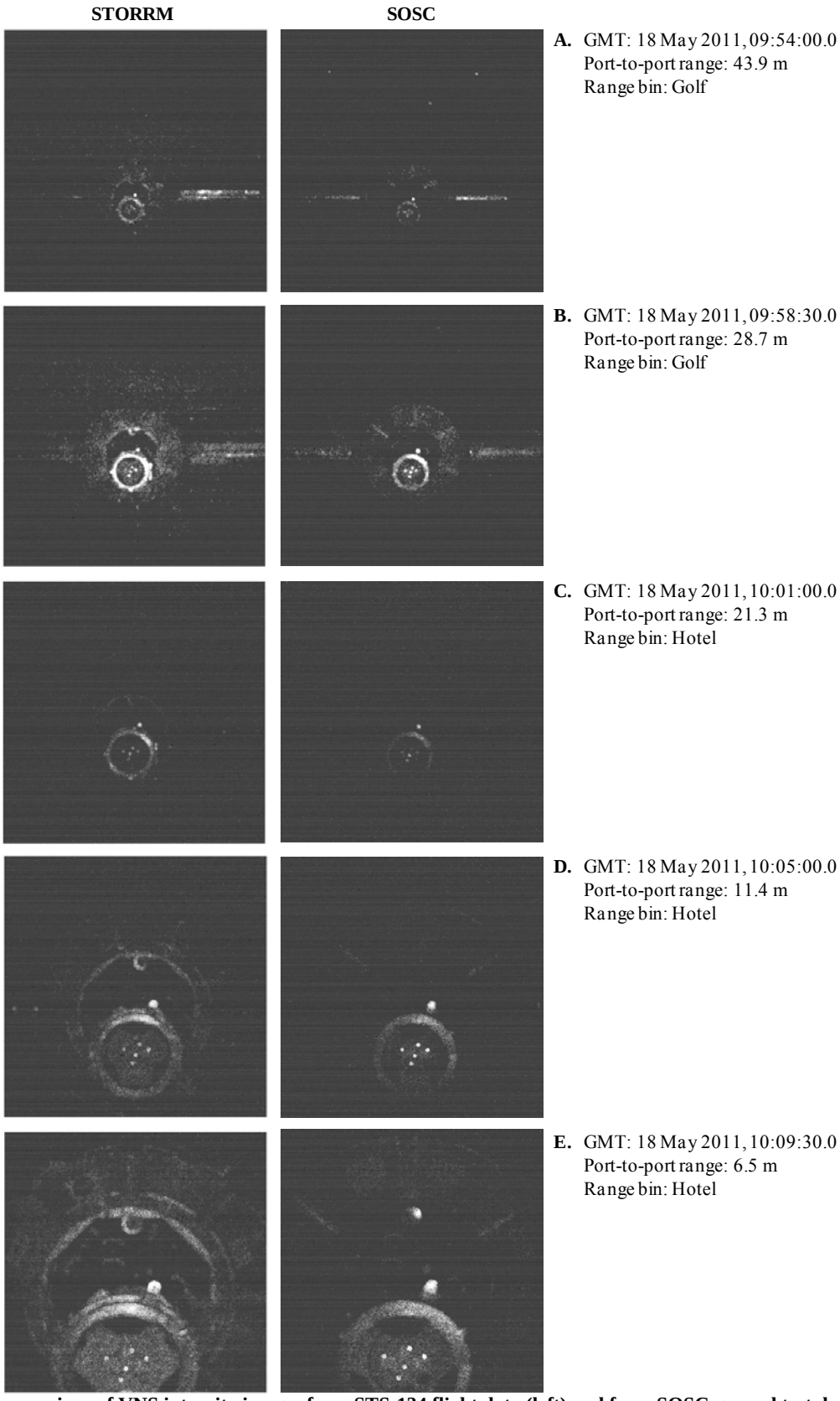

Figure 17. Comparison of VNS intensity images from STS-134 flight data (left) and from SOSC ground test data (right).

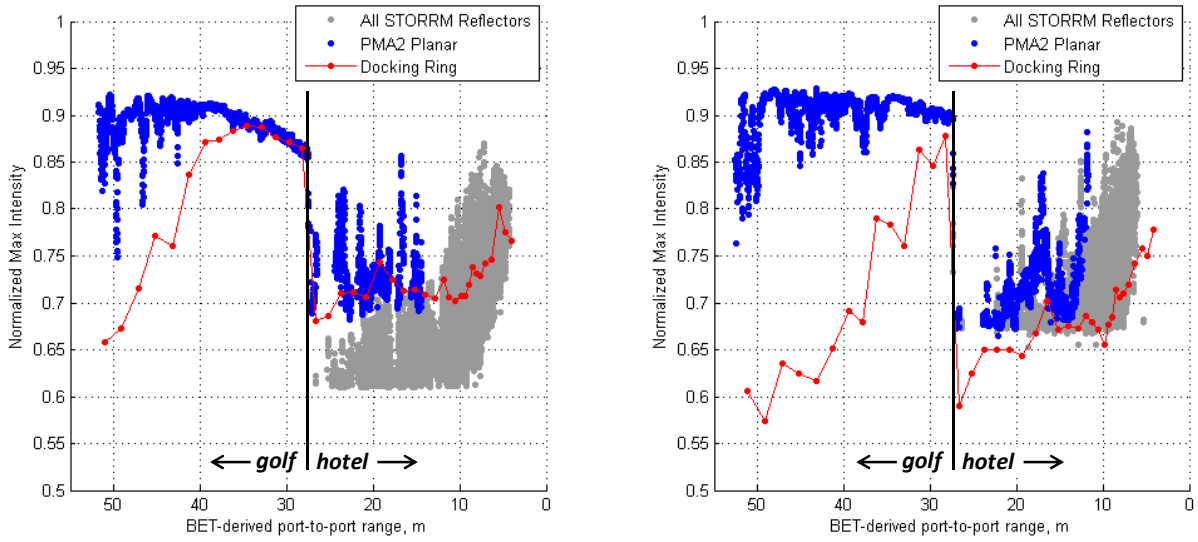

a) STORRM data from STS-134 FD3 rendezvous *b) Simulated rendezvous in SOSC*

Figure 18. Numerical comparison of VNS intensity returns from the reflectors and docking ring observed in STS-134 flight data (left) and in SOSC ground test data (right).

VIII. Conclusions

This paper presented a comparison of VNS data collected from: (1) on-orbit during the STORRM DTO on STS-134 and (2) on the ground during a re-creation test of the STS-134 rendezvous in the SOSC in Colorado. First, summaries of the STORRM DTO and the SOSC test facility were presented. Each of these tests (both flight and ground) have met most of their test objectives. After comparing the data, results indicate that the ground test facility accurately re-creates the nature of the reflector returns seen on-orbit, thus making the facility suitable for testing the navigation performance of the VNS. That being said, a great deal of forward work still exists to accurately simulate the spurious reflections from the ISS that were seen on-orbit. These spurious reflections are the primary source of difficulty in using Flash LIDAR images containing reflectors and are important to model if the ground test facility is to be used to demonstrate system robustness.

IX. Acknowledgements

The authors thank the other members of the Orion MPCV team who participated in STORRM and the SOSC re-creation tests. Specifically, we thank Chris D'Souza, Pete Spehar, Scott Cryan, and Howard Hu of the NASA Johnson Space Center; Angie Kibler of Lockheed Martin; and Fred Clark, Renato Zanetti, and Zoran Milenkovic of the C.S. Draper Laboratories. We also thank the SOSC team at Lockheed Martin who made the re-creation test possible, especially John Bendle, David Huish, Reid Hamilton, and Frank Moore.

References

1. Miller, K., Masciarelli, J., Rohrschneider, R., and Gravseth, I., "Critical Advancement in Telerobotic Servicing Vision Technology," *AIAA SPACE 2010 Conference & Exposition*, Anaheim, CA, 30 Aug - 2 Sept 2010.
2. Christian, J., Hinkel, H., D'Souza, C., Maguire, S., and Patangan, M., "The Sensor Test for Orion RelNav Risk Mitigation (STORRM) Development Test Objective," *AIAA Guidance, Navigation, and Control Conference*, Portland, OR, 8-11 Aug 2011.
3. Nguyen, T., Goodwin, P., Ernst, D., Jouppi, N., and Tichenor, M., "Exploration Testbeds – Industry Investments Supporting Project Constellation Risk Reduction," *AIAA SPACE 2009 Conference & Exposition*, Pasadena, CA, 14-17 Sept 2009.
4. D'Souza, C., Milenkovich, Z., Wilzon, Z., Huish, D., Beldle, J., and Kibler, A., "Space Operations Simulation Center and Closed-loop Hardware Testing for Orion Rendezvous System Design," *AIAA Guidance, Navigation, and Control Conference*, Minneapolis, MN, 2012.
5. Foix, S., Alenya, G., and Torras, C., "Lock-in Time-of-Flight (ToF) Cameras: A Survey," *IEEE Sensors Journal*, Vol. 11, No. 9, September 2011, pp 1917-1926.
6. Stuit, T., "Designing the STS-134 Re-Rendezvous:A Preparation for Future Crewed Rendezvous Missions," *AIAA Space 2011 Conference & Exposition*, Long Beach, CA, 27-29 September 2011.
7. Gonzalez, R. and Woods, R., *Digital Image Processing, 3rd Ed.*, Pearson Prentice Hall, Upper Saddle River, NJ, 2008.
8. Breen, E., and Jones, R., "Attribute Openings, Thinnings, and Granulometries," *Computer Vision and Image Understanding*, Vol. 64, No. 3, November 1996, pp 377-389.
9. Gravseth, I., Rohrschneider, R., and Masciarelli, J., "Vision Navigation Sensor (VNS) Results from the STORRM Mission," *AAS Guidance and Control Conference*, Breckenridge, CO, 3-8 February 2012.
10. Ma, Y., Soatto, S., Koecka, J., and Sastry, S., *An Invitation to 3-D Vision: From Images to Geometric Models*, Springer, New York, NY, 2010.